Modeling and Analysis of a Battery Energy Storage System Supplied from Photovoltaic Power Source

YAGMUR KIRCICEK, AHMET AKTAS, MEHMET UCAR[1],
SULE OZDEMIR, ENGIN OZDEMIR

Department of Energy Systems Engineering / Faculty of Technology / Kocaeli University
Umuttepe Campus, 41380, Kocaeli
[1]Deparment of Electrical and Electronics Engineering / Faculty of Engineering / Duzce University
Konuralp Campus, 81620, Duzce
yagmurkircicek@hotmail.com, ahmet_aktas_1987@hotmail.com, mehmetucar@duzce.edu.tr
sozaslan@kocaeli.edu.tr, eozdemir@kocaeli.edu.tr

Abstract: The biggest challenge with combining renewable energy into the electrical power system is the fact that the produced energy is intermittent. Solar energy is only available for usage when the sun is out and the sky is clear. A battery energy storage system (BESS) can solve this intermittency problem. The battery energy storage is necessary to help get a stable and reliable output from photovoltaic (PV) power generation system for loads and improve both steady and dynamic behaviors of the whole power system. Integrating the BESS with renewable energy sources can make the intermittent renewable energy sources more dispatchable. In this paper, modeling and analysis of the BESS for integrating intermittent renewable energy resources with energy storage for 3-phase 4-wire grid-connected electrical power systems is proposed. The BESS will play a vital role for integrating renewable energy into power system. Because renewable energy is not constant (aside from hydroelectricity) and is intermittent, this type of energy needs to be conserved and used at appropriate times. This paper investigates a capacity sizing calculation of the BESS supported by renewable energy source supplied from photovoltaic power. The paper presents detailed transient models of the grid-connected PV/battery power generation system, and all these models are simulated by using MATLAB/Simulink.

Keywords: Photovoltaic panels, Battery energy storage system, 3-phase 4-wire grid-connected, DC/DC converter, DC/AC inverter.

NOMENCLATURE

I_{PV}	Cell current (A)
I_{ph}	Photocurrent (A)
I_d	Internal diode current (A)
I_p	Shunt current across the p-n junction (A)
I_0	Saturation current (A)
V_d	Diode voltage (V)
K	Boltzmann constant
F	Solar cell ideality constant
q	Electron charge
T_{PV}	Temperature of the cell (^oC)
R_s	Resistance connected in series (Ω)
R_p	Resistance connected in parallel (Ω)
N_p	Parallel solar cells
N_s	Series solar cells
V_{oc}	Open circuit voltage (V)
I_{sc}	Short-circuit current (A)
MPP	Maximum power point
I_{Lm}	Current across the load at the maximum power point (A)
V_{Lm}	Voltage across the load at the maximum power point (V)
V_{OCV}	2nd-order Randle model voltage (V)
SOC	Battery state of charge
DOC	Deep of charge
R_1 and C_1	Associated with the battery of SOC
R_2 and C_2	Associated with the battery of DOC
V_{BAT}	Battery voltage (V)
V_{OCV}	Battery voltage generator (V)
I_{BAT}	Battery current (A)
C_n	Battery capacity (F)
$C(i_{avg})$	Current-dependent battery capacity
E_0	Open circuit voltage (V)
R_{10}	1st RC branch constant in (Ω)
$\tau 1$	1st RC branch time constant
R_{20}	2nd RC branch constant in (Ω)
$\tau 2$	2nd RC branch time constant
v_{gabc}	Grid Voltage (V)

v_{pv}	PV Voltage (V)
v_{dc}	DC Link Voltage (V)
v_{bat}	Battery Voltage (V)
i_{gabcn}	Grid Current (A)
i_{Labcn}	Load Current (A)
i_{iabcn}	Inverter Current (A)
i_{pv}	PV Current (A)
i_{boost}	Boost Current (A)
i_{bat}	Battery Current (A)
i_{bid}	Bidirectional Current (A)

1. INTRODUCTION

It is possible to store energy in large scale using water dams or fuel reservoirs. Ideally, when using electricity it has to be produced as it is being consumed. Unfortunately, the photovoltaic energy has to be stored since during the night or periods of cloudy days there is not enough production of electricity. Energy storage then becomes an essential item to assure a continuous power supply. The most widely used means of storage for PV systems is the battery bank, because it is inexpensive and simple to manufacture, it has a mature, reliable, and well-understood technology and when used correctly, is durable and provides a dependable service. Its self-discharge is relatively low and demands for low maintenance requirements with high charge/discharge rates [1,2].

Battery energy storage system is utilized to smooth the output fluctuation of the entire hybrid system. Energy management of the entire system and energy flow between systems and grid are based on power electronics interface. The BESS mitigates fluctuating power generated from the PV array, and injects more stable (less fluctuating) power output into the grid. The purpose is to smooth power fluctuation of the renewable energy sources and so transfer more stable power into the grid. This improves the quality of power delivered to the grid. This mode of operation reduces the voltage and harmonic variation at the point of common coupling with the grid [3].

In this paper, PV array is first connected to the common DC bus by a boost converter, where the battery is also connected with a bi-directional DC/DC converter, and then integrated into the alternating current (AC) utility grid by a common DC/AC inverter. Maximum power point tracking (MPPT) helps PV array to generate the maximum power to the grid, and the battery energy storage can be charged and discharged to balance the power between PV generation and utility grid. (4) In Section 2, the analytical modeling of PV and battery with model validation results are briefly presented. Section 3 shows the 3-phase 4-wire grid-connected PV/BESS configuration. In Section 4, modeling and simulation are implemented using MATLAB/Simulink and SimPowerSystems software packages to verify the effectiveness of the proposed system.

2. PV ARRAY AND BATTERY MODELS

2.1. PV Array Model

Photovoltaic cells consist of a p-n junction fabricated in a thin wafer or layer of semiconductor. There are many kinds of solar cells in different materials. The common material is monocrystalline silicon or polycrystalline silicon. The ideal solar cell is the one in which a current source is connected in antiparallel with a diode as shown in Fig. 1. When the cell is exposed to sunlight, the direct current generated which varies linearly with solar radiation. The model can be improved, including the effect of a shunt resistance and series resistance. The equivalent circuit of the single-diode model for PV cells is shown in Fig. 1.

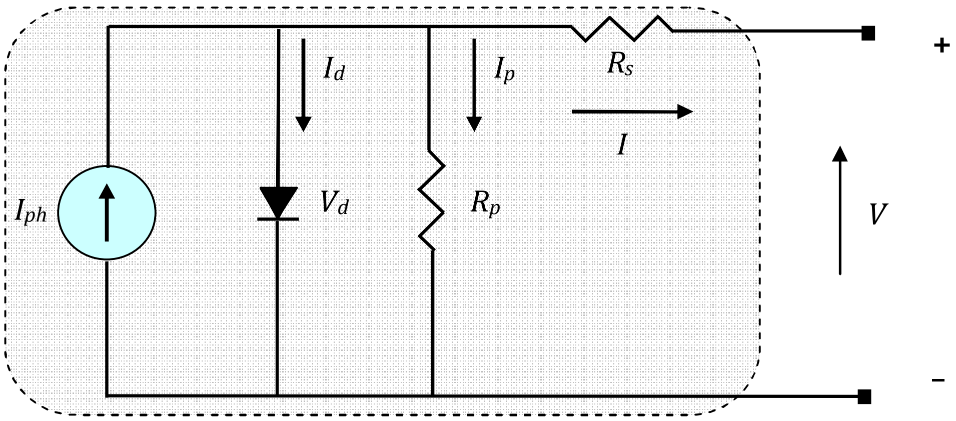

Fig.1 Equivalent circuit of a photovoltaic cell based on the single-diode model

The output current of a PV panel can be derived from the Kirchhoff's law, to give $I_{PV} = I_{ph} - I_d - I_p$ where I_{PV} is the cell current, I_{ph} is the photocurrent, I_d is the internal diode current and I_p is the shunt current across the p-n junction [5,6].

PV module consists of PV cells connected in a given way in parallel or series depending on the PV module ratings. A single module rating is limited to few hundred watts. When higher power is required PV modules are connected in series and in parallel to obtain PV array. The theoretical model of a PV array is deducted from that of a single PV cell.

The general current and voltage of the solar cell is given as follows:

$$I_{PV} = I_{ph} - I_d - I_p = I_{ph} - I_o\left[e^{\left(\frac{qV_d}{KFT_{PV}}\right)-1}\right] - \frac{V_d}{R_p} \tag{1}$$

Where, I_0 is saturation current, V_d is diode voltage expressed in volts, K is Boltzmann constant, F is solar cell ideality constant, q is electron charge, T_{PV} is temperature of the cell, R_s is resistance connected in series, R_p is resistance connected in parallel. The equivalent circuit for the solar cells arranged in N_p parallel and N_s series is shown in Fig. 2, array current and array voltage becomes:

$$I_{PV} = N_p I_{ph} - I_o \left[e^{\left(\frac{q\left(\frac{V_d}{R_s} + \frac{IR_s}{R_p} \right)}{N_s KFT_{PV}} \right)} - 1 \right] - \frac{N_p V_d / N_s}{R_p} \tag{2}$$

Where N_p represents the number of parallel modules. Note that each module is composed of N_s cells connected in series. N_s, I_{ph} corresponds to the short circuit current of the solar array.

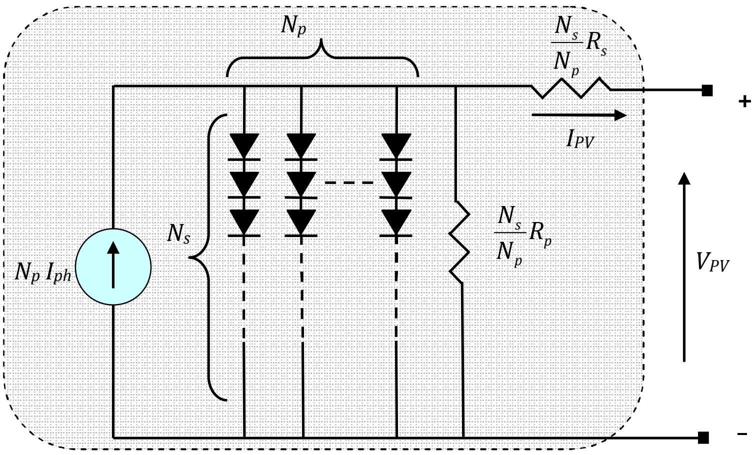

Fig. 2 Electrically equivalent of solar array circuit

Without other losses, there is a theoretical maximum power point expected from PV solar panels and that value would occur at the open circuit voltage V_{oc} and short-circuit current I_{sc}. Such maximum value cannot be achieved in practical cases, so a numerical factor is created to estimate how close the production capability of a panel can go. This is called the fill factor defined as:

$$FF = \frac{I_{Lm} V_{Lm}}{I_{sc} V_{oc}} \tag{3}$$

Where, I_{Lm} and V_{Lm} are the current through and voltage across the load at the maximum power point (MPP). The fill factor shows how well module P-V characteristic suits in a rectangle of V_{oc} length and I_{sc} width [7-9].

2.2. Battery Model

Batteries are the main storage technology used in PV systems. Many different types of battery models have been developed for different application areas. For example, the electrochemical models are used in battery design. These models describe the battery in its very detail using a set of six coupled differential equations. Another example is the electrical circuit models used in electrical engineering, which focus on the electrical properties of the battery. Although these models describe the battery accurately. A simple equivalent circuit battery model is shown in Fig. 3. A variety of models exist that predict battery behavior to varying degrees of accuracy. The circuit models the internal resistance and transient behavior of the battery using a series resistance and two branch RC circuits [10-12].

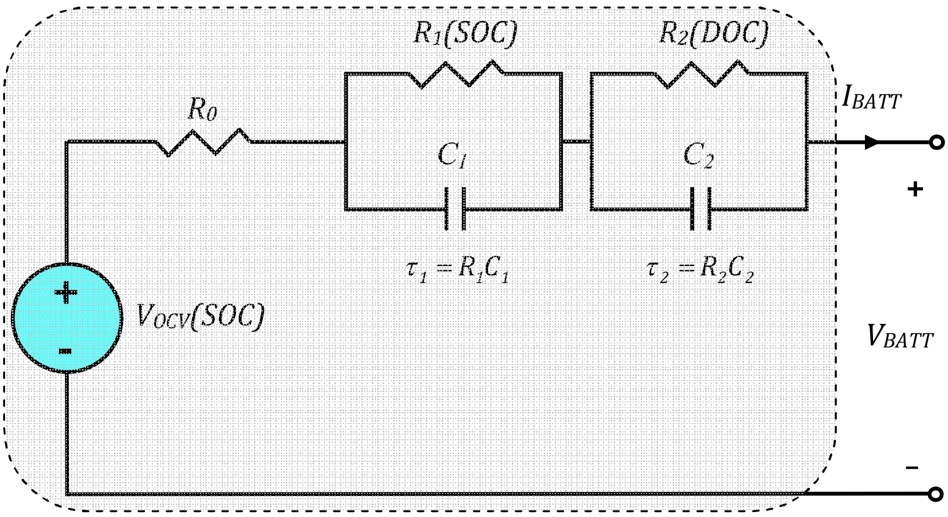

Fig.3 Equivalent circuit of second order Randle's model

The Fig. 3 represents the 2nd-order Randle's model circuit where R_o is the internal resistance of the battery's terminals and inter-cell connections. The other resistances and capacitors are used to model the cell dynamics. The battery model takes into account the battery state of charge (SOC) and deep of charge (DOC). Where, first branch R_1 and C_1 is associated with the battery of SOC, the second branch R_2 and C_2 is associated with the battery's DOC. Furthermore, the 2nd-order Randle model voltage generator (V_{OCV}) models the open circuit voltage (which is the voltage of the cell when it is rested) as a function of SOC. It depends on SOC, temperature and also the device design. The battery voltage obtained is given by;

$$V_{BATT} = V_{OCV}(SOC) - I_{BATT}\left(R_0 + \frac{R_1}{1 + sR_1C_1} + \frac{R_2}{1 + sR_2C_2} \right) \tag{4}$$

$$V_{BATT} = V_{OCV}(SOC) - I_{BATT}R_0 - I_{BATT}\left(\frac{K(1 + sK_1)}{(1 + sK_2)(1 + sK_3)} \right) \tag{5}$$

$$R_1 = R_{10} e(-K_1(1-SOC)) \quad (6)$$

$$R_2 = \frac{R_{20}}{DOC} \quad (7)$$

$$SOC = 1 - \frac{1}{C_n} \int I_{BATT} d\tau \quad (8)$$

$$DOC = 1 - \frac{1}{C(i_{avg})} \int I_{BATT} d\tau \quad (9)$$

Where, V_{BAT} is battery voltage V, V_{OCV} is battery voltage generator V, I_{BAT} is battery current A, SOC is the state of charge of the battery, DOC is the deep of charge of the battery, C_n is the battery capacity, $C(i_{avg})$ is the current-dependent battery capacity, E_0 is the open circuit voltage when the battery is fully charge, R_{10} is the 1st RC branch constant in Ω, $\tau 1$ is the 1st RC branch time constant in sec, $K1$ is a constant, R_{20} is the 2nd RC branch constant in Ω, $\tau 2$ is the 2nd RC branch time constant in sec [13-15].

Several parameters characterize the performance of a battery; self-discharge resistance: it is the resistance that is associated with the electrolysis of water at voltage levels and slow leakage across the battery terminal at low voltage. This resistance is more temperature sensitive and is inversely proportional to the temperature. Charge and discharge resistance: these resistances are associated with the electrolyte resistance, plate resistance, and fluid resistance; and these resistances vary during charging and discharging. Overcharge and over discharge resistance: these resistances are attributed largely to the electrolyte diffusion during over charging and over discharge. Rate of charge and discharge: to extend service life of the battery, the rate of charge or discharge should not be too high. Also the frequency of charge and discharge cycles affects the battery life significantly. The frequency of switching between charge and discharge is especially high in battery energy storage system which drastically reduces the life of the battery [16].

3. GRID CONNECTED PV POWER GENERATION AND BESS

Battery energy storage systems (BESS) will most likely play an important role in enabling integration of small scale renewable energy sources, from residential and 3-phase 4-wire grid connected power systems, into the electricity networks. This paper focuses on electrical energy storage systems, especially battery energy storage systems for 3-phase 4-wire grid connected electrical power systems [4].

In order to operate the distributed power supply system in an autonomous mode with a high efficiency and to ensure an effective continual power supply throughout the year, an energy storage element is always required as an energy buffer. Furthermore, it also has a significant impact upon improving power quality of distributed generation systems. In this study, the lead acid battery is used in energy storage unit. Traditionally, the lead acid battery is the most popular energy storage device due to its low cost and wide availability [19].

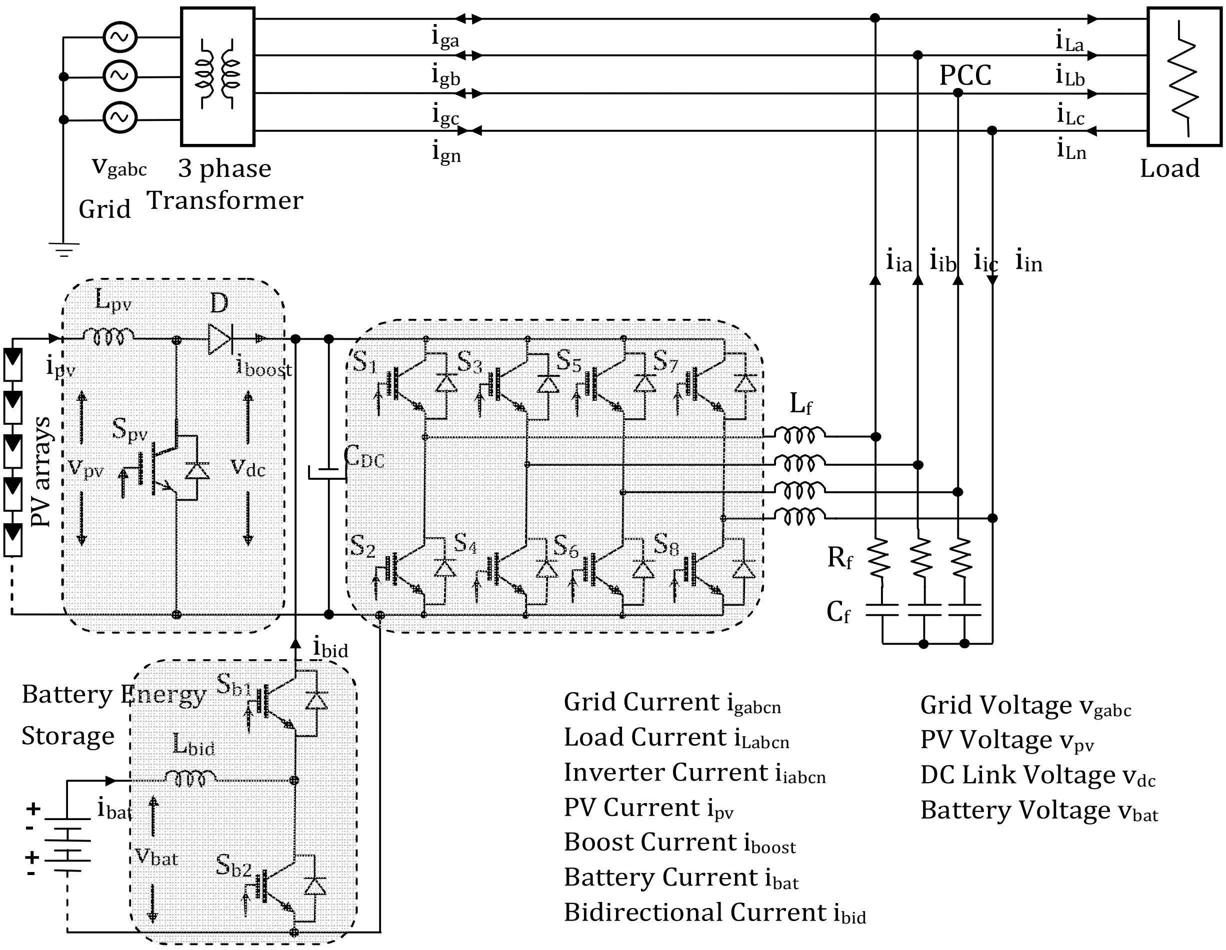

Fig.4 3-phase 4-wire grid-connected PV /battery generation system

Fig. 4 shows the configuration of the 3-phase 4-wire grid-connected PV/Battery power generation system. PV array and battery are connected to the common DC link via a DC/DC boost converter and DC/DC bidirectional converter respectively, and then interconnected to the AC grid via a common DC/AC inverter. For the two-stage PV system, the maximum power point tracking is realized by controlling the DC/DC boost converter [15]. The DC/DC boost converter (step up) serves the purpose of transferring maximum power from the solar PV module to the DC link. The DC/DC boost converter acts as an interface between the 3-phase 4-wire inverter. By changing the duty cycle, the load impedance as seen by the source is varied and matched at the point of the peak power with the source so as to transfer the maximum power [17,18].

In distributed generation system applications, the batteries and the DC link at different voltage batteries are at low voltage levels and DC link at high voltage levels to have higher efficiency on the grid connected generation systems. Only buck and boost converter do not have bidirectional power flow capability. Therefore DC/DC converter used to bi-directional so that the energy can flow from the battery to the DC link and from DC link to the battery [20].

4. SIMULATION RESULTS

The MATLAB/Simulink model consist of an array of PV cells and DC/DC boost converter, a battery group and bidirectional DC/DC converter, associated with the grid a constant load and 3-phase 4-wire grid-connected inverter. Fig. 5 presents the simulation model used to assess the above mentioned components.

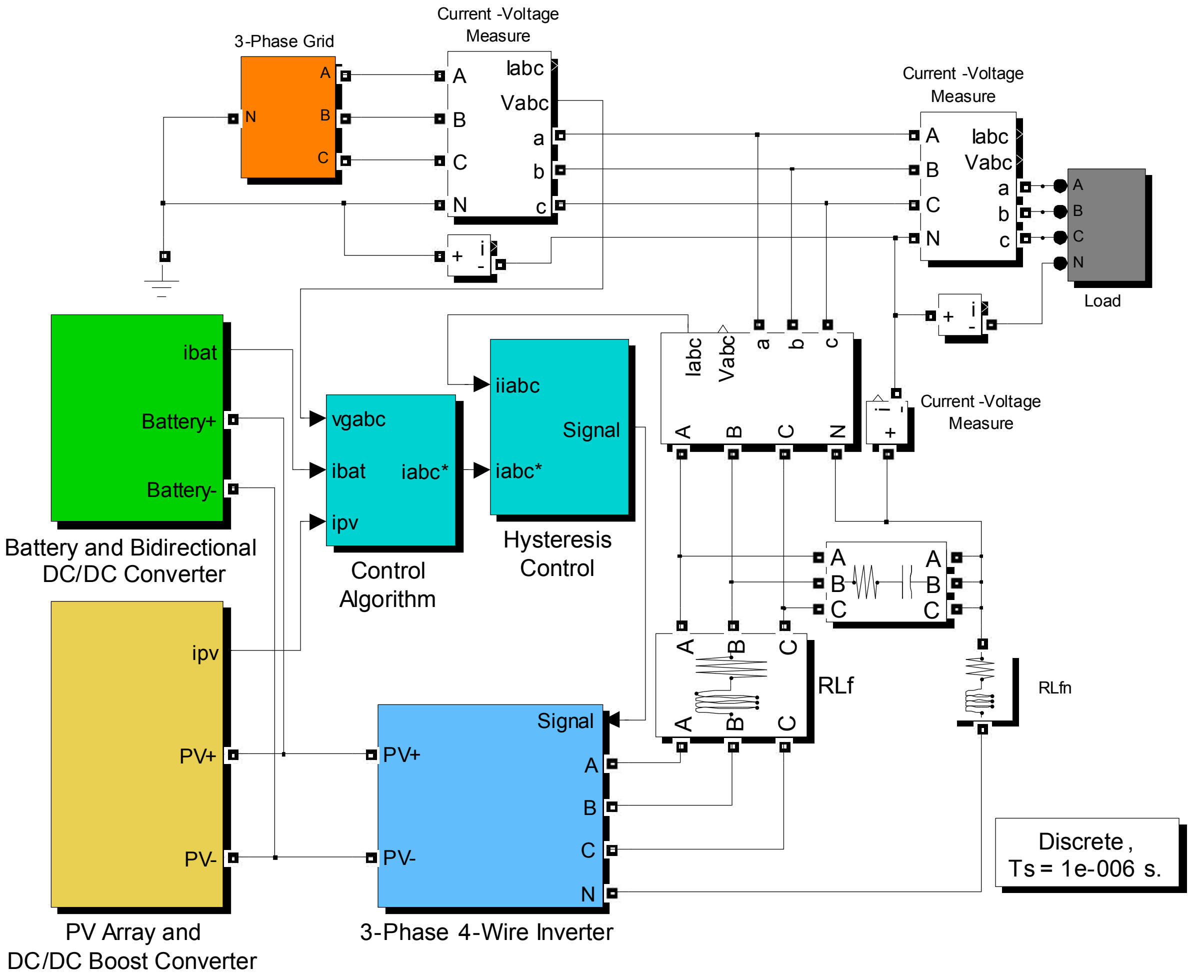

Fig.5 Simulation model of 3-phase 4-wire grid-connected PV/BESS

PV array, grid, battery and load parameters used in the simulation model are given in Table 1. PV array was simulated radiation under 1000W/m^2 aggregate power 4000 W. Also 105 Ah lead-acid battery type is selected in this study. In simulation, the results are taken depending on SOC of the battery and radiation of the PV by connecting the constant load.

Table 1 System parameters

Parameters		
PV Array	Open Circuit Voltage (V_{oc})	228.9 V
	Short Circuit Current (I_{sc})	23 A
	Voltage at MPP ($V_{\max}$)	185.25 A
	Current at MPP ($I_{\max}$)	21.6 A
Grid	Voltage (v_{gabc})	110 V_{rms} /L-N
	Frequency (*f*)	50 Hz
	Impedance (R_f , L_f)	10mΩ, 59μH
Battery	Battery Type	Lead-Acid
	Nominal Voltage (v_{bat})	120 V
	Rated Capacity (Ah)	105 Ah
Load	Resistance	19.37 Ω

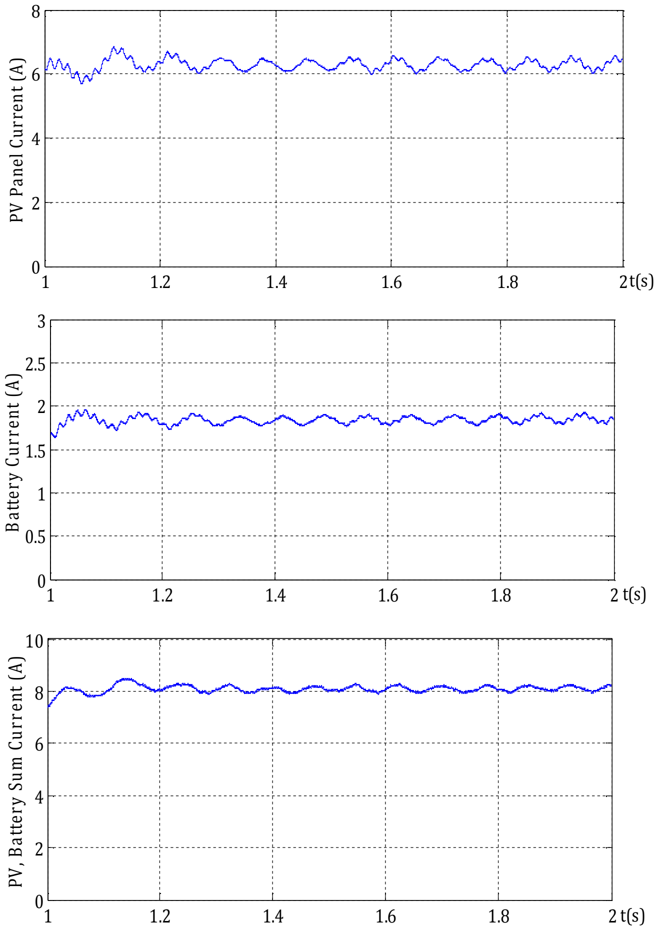

Fig.5 $P_{pv} < P_{load}$ in case, PV panel, battery and PV+battery currents respectively

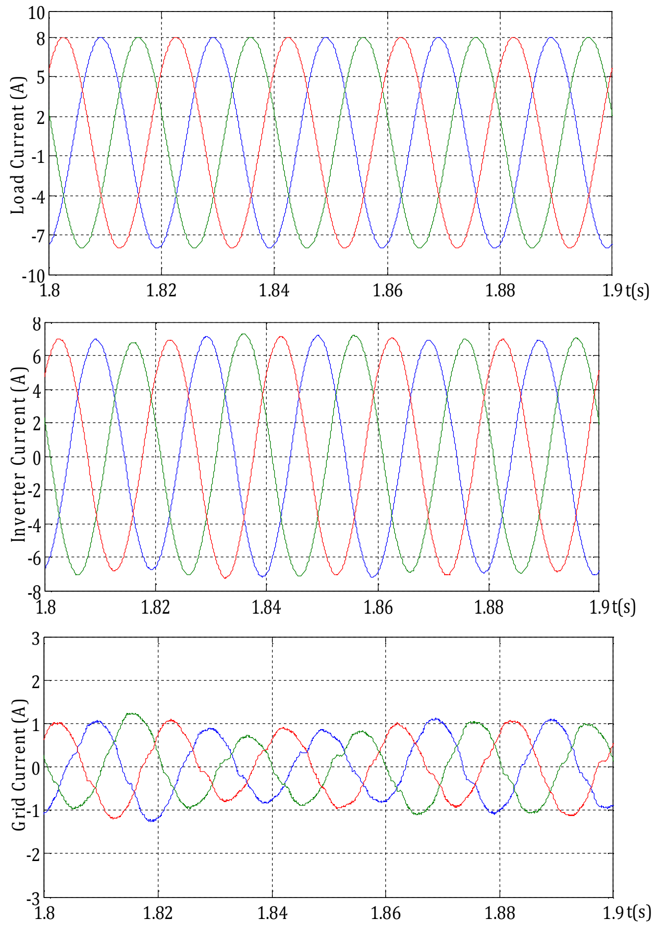

Fig.6 $P_{pv} < P_{load}$ in case, load, inverter and grid currents respectively

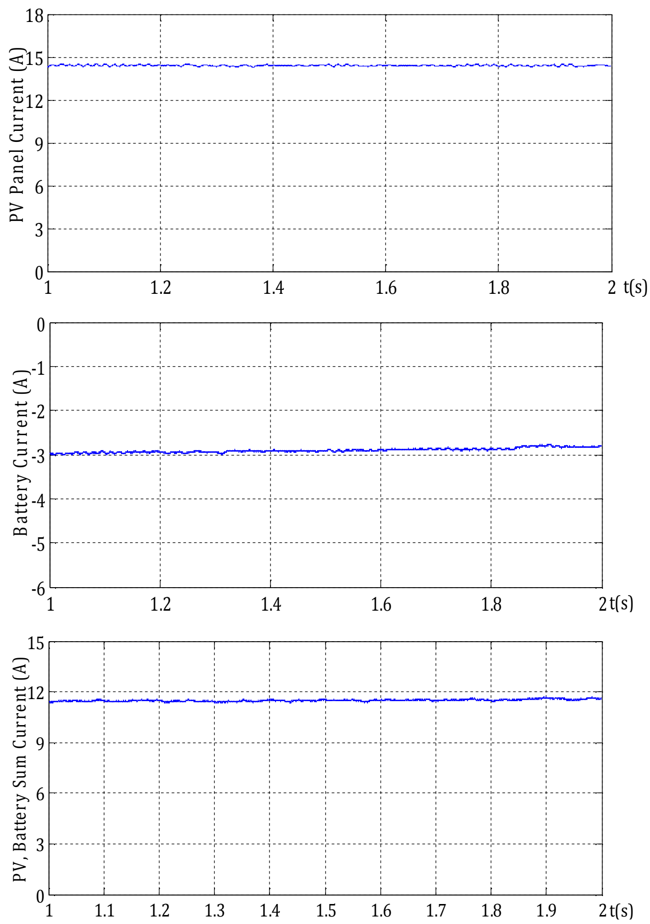

Fig.7 $P_{pv} > P_{load}$ in case, PV panel, battery and PV+battery currents respectively

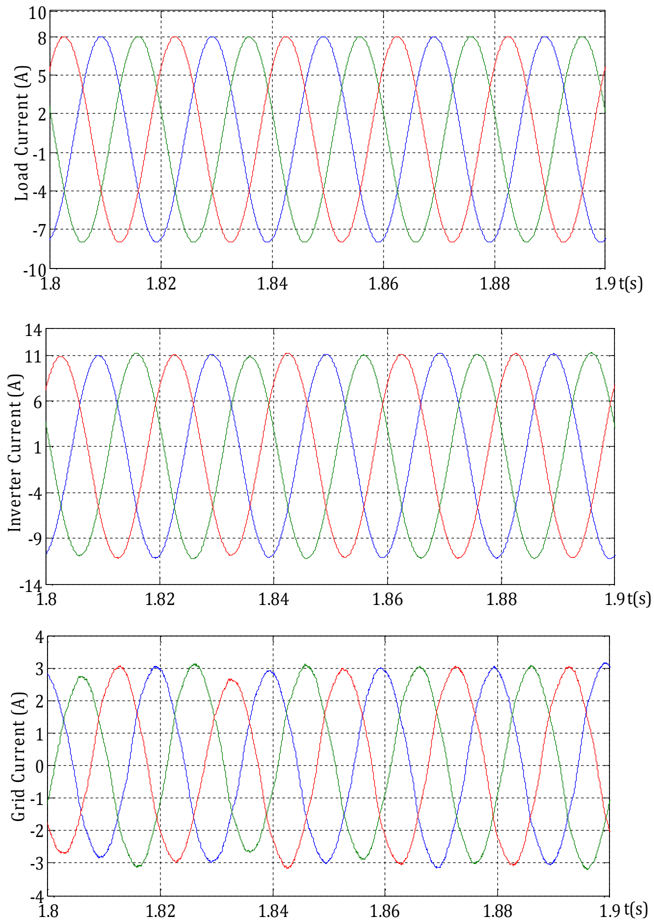

Fig.8 $P_{pv} > P_{load}$ in case, load, inverter and grid currents respectively

In this study, two operating conditions were simulated. Fig. 5 and 6 and Fig. 7 and 8 shows this two conditions waveform. The first case, $P_{pv} < P_{load}$ when in other cases $P_{pv} > P_{load}$. PV power is smaller than load power ($P_{pv} < P_{load}$) in operation mode, PV generated power to feed directly to the load and power demanded by the load DC/DC bidirectional converter supplied with the help of the battery. PV power is higher than load power ($P_{pv} > P_{load}$) in operation mode on demand that to ensure, batteries DC/DC bidirectional converter in buck mode to recharge running and the remaining energy is transferred to the grid.

5. CONCLUSION

Solar, wind and other renewable energy sources are becoming an important part of energy supply to the power grid. In this study, grid connected PV/BESS based distributed generation system was modeled and analyzed. The proposed system, composed of PV panel, battery energy storage, DC/DC bidirectional and boost converter, 3-phase 4-wire grid-connected inverter models and control methods, was simulated in MATLAB/Simulink. The DC/DC boost converter was connected to PV panels and operated at MPP. The BESS can be charged or discharge by using the DC/DC bidirectional converter to maintain the power balance between PV power generation and the load demand. Simulation results prove that the grid-connected PV/BESS generation system improves the PV utilization and provides stable and reliable power for loads or power grid during its operation modes.

6. Acknowledgements

This paper was supported by within TUBITAK project number of 113E143.

7. References

[1] Femia, N., Petrone, G., Spagnuolo, G., Vitelli, M., Power Electronics and Control Techniques for Maximum Energy Harvesting in Photovoltaic System, CRC Press, 2012, pp. 1-87

[2] Barnes, F. S., Levine, J. G., Large Energy Storage Systems Handbook, CRC Press, 2011, pp. 61-109

[3] Jeon, J., Kim, S., Cho, C., Ahn, J., Kim, J., Power Control of Grid-Connected Hybrid Generetion System with Photovoltaic/Wind Turbine/Battery Sources, The 7th International Conference on Power Electronics, 22-26 October, 2007, Daegu, pp. 506-510

[4] Garimella, N., Nair, N. C., Assessment of Battery Energy Storage Systems for Small Scale Renewable Energy Integration, IEEE TENCON Region 10 Conference, 23-26 January, 2009, Singapore, pp. 1-6

[5] Panda, B., Das, S., Panda, B., MATLAB/SIMULINK Based Modeling of Solar Photovoltaic Module, International Congress on Renewable Energy (ICORE), Excel India Publishers, India, 2013, pp. 228-235

[6] Amatoul, F. Z., Lamchich, M. T., Outzourhit, A., Design Control of DC/AC Converter for a Grid Connected PV Systems with Maximum Power Tracking Using MATLAB/SIMULINK, International Conference on Multimedia Computing and Systems (ICMCS), 7-9 April, 2011, Ouarzazate, pp. 1-6

[7] Şahin, M. E., Okumuş, H. İ., Modeling and Simulation of Solar Cell Module in Matlab/Simulink, The Journal of Electrical, Electronics, Computers and Biomedical Engineering, Vol.3, No.5, 2013, pp. 17-25

[8] Sera, D., Real-time Modelling, Diyagnostic and Optimised MPPT for Residential PV systems, Aalborg University, Institute of Energy Technology, Denmark, 2009, pp. 3-74

[9] Aktas, A., 3 Phase 4 Wire For Photovoltaic Systems Network Connection Maximum Power Point Tracking 4 Leg Inverter Design, MSc Thesis, Kocaeli University, Graduate School of Natural and Applied Sciences, Faculty of Technology, Department of Energy Systems Engineering, Kocaeli, 2013, pp. 8-52

[10] Codeca, F., Savaresi, S. M., Rizzoni, G., On battery State of Charge Estimation: A New Mixed Algorithm, 17th IEEE International Conference on Control Applications, 3-5 September, 2008, Texas, pp. 102-107

[11] Jackey, R. A., A Simple, Effective Lead-Acid Battery Modeling Process for Electrical System Component Selection, The MatWorks Incorporated, 2007, pp. 1-9

[12] Xiong, X., Chi, K., Ruan, X., Bifurcation Analysis of Standalone Photovoltaic-Battery Hybrid Power System, IEEE Transactions on Circuits and Systems 1, Vol.60, No.5, 2013, pp. 1354-1365

[13] Glavin, M. E., Paul, K. W., Armstrong, S. , Hurley, W. G. , A Stand-alone Photovoltaic Supercapacitor Battery Hybrid Energy Storage System, 13th Power Electronics and Motion Control Conference, 1-3 September, 2008, Poznan, pp. 1688-1695

[14] Tremblay, O., Dessaint, L. A., Experimental Validation of a Battery Dynamic Model for EV Applications, EVS24 International Battery, Hybrid and Fuel Cell Electric Vehicle Symposium, 13-16 May, 2009, Stavanger, pp. 1-10

[15] Ding, F., Li, P., Gao, F. , Ding, C., Wang, C., Modeling and Simulation of Grid-connected Hybrid Photovoltaic/Battery Distributed Generation System, 2010 China International Conference on Electricity Distribution, 13-16 September, 2010, Nanjing, pp. 1-10

[16] Chiasson, J., Variamohan, B., Estimating The State of Charge of a Battery, IEEE Transactions on Control Systems Technology, Vol.13, No.3, 2005, pp. 465-470

[17] Baoquan, L., Fang, Z., Xianwen, B., Control Method of the Transient Compensation Process of a Hybrid Energy Storage System Based on Battery and Ultra-Capacitor in Micro-grid, IEEE International Symposium on Industrial Electronics (ISIE), 28-31 May, 2012, Hagzhou, pp. 1325-1329

[18] Adhikari, S., Li, F., Coordinated V-f and P-Q Control of Solar Photovoltaic Generators with MPPT and Battery Storage in Microgrids, IEEE Transactions on Smart Grid, No.99, 2014

[19] Jiancheng, Z., Liantao, J., An Effective Hybrid Energy Storage System Based on Battery-EDLC for Distributed Generation Systems, 5th IEEE Conference on Industrial Electronics and Applications (ICIEA), 2010, Taichung, pp. 819-824

[20] Dutta, D., Ganguli, S., Design of A Bidirectional Dc-Dc Converter for Hybrid Electric Vehicles (HEV) Using Matlab, International Journal of Advanced Research in Electrical, Electronics and Instrumentation Engineering, Vol.2, No.7, 2013, pp. 2994-3002